RSC Advances

Bio-electrocatalyzed electron efflux in Gram positive and Gram negative bacteria: An insight on disparity in electron transfer kinetics

Journal:	*RSC Advances*
Manuscript ID:	RA-ART-04-2014-003489.R2
Article Type:	Paper
Date Submitted by the Author:	17-Apr-2014
Complete List of Authors:	Annie Modestra, Jampala; Indian Institute of Chemical Technology, Bioengineering and Environmental Sciences Venkata Mohan, S; Indian Institute of Chemical Technology, Bioengineering and Environmental Sciences

Bio-electrocatalyzed electron efflux in Gram positive and Gram negative bacteria: An insight on disparity in electron transfer kinetics

J. Annie Modestra and S Venkata Mohan*

Bioengineering and Environmental Sciences (BEES), CSIR-Indian Institute of Chemical Technology (CSIR-IICT), Hyderabad-500 007, India

* E-mail: vmohan_s@yahoo.com; Tel/Fax: 0091-40-27191664

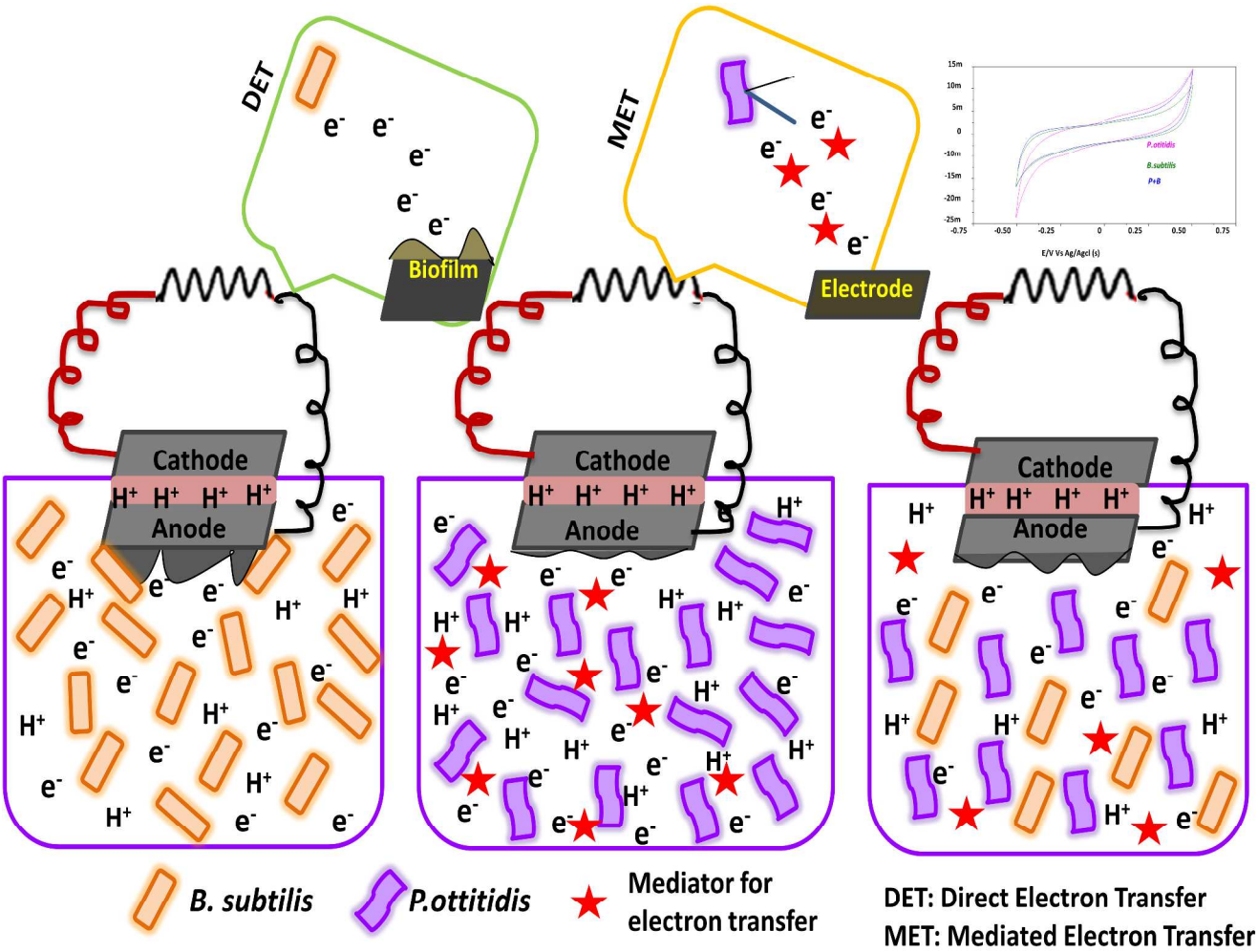

Bio-electrocatalyzed electron efflux in Gram positive and Gram negative bacteria: An insight on disparity in electron transfer kinetics

J. Annie Modestra and S. Venkata Mohan*

Bioengineering and Environmental Sciences (BEES), CSIR-Indian Institute of Chemical Technology (CSIR-IICT), Hyderabad-500 007, India

*** E-mail: vmohan_s@yahoo.com; Tel/Fax: 0091-40-27191664**

Abstract

Electron transfer (ET) behavior of bacteria varies significantly in a bio-electrocatalyzed environment. However, exact mechanisms of ET towards electrodes are not well defined in most electrochemically-active microorganisms. The bacterial cell structure and composition affects the electron transfer properties apart from their growth. In the present study, disparity in ET between gram positive (GPB, *Bacillus subtilis*) and gram negative (GNB, *Pseudomonas otitidis*) bacteria (both differ in chemical and physical properties of cell wall/structure) and combination of both (GPB+GNB) was evaluated individually in bio-electrochemical cells (BEC_B, BEC_P and BEC_{P+B}). *P. otitidis* being a GNB exhibited mediated electron transfer (MET) through the redox shuttles detected as a peak in derivative of CV (DCV) analysis with an extra cellular electron transfer (EET) site potential of -36 mV corresponding to the phenazine derivative. GPB, *B. subtilis* exhibited direct electron transfer (DET) through the membrane bound proteins with peak potentials of 0.04 V, 0.211 V and 0.423 V that correspond to cytochrome-C, bc1 and aa3. Electron transfer capabilities in terms of electron transfer rate (K_{app}; 81 s^{-1}), redox catalytic currents (OC: 40 mA; RC: -50 mA), power density (63.3 mW/m^2), sustainable anodic resistance (5 kΩ) and currents (5 mA) were found to be higher in GNB in comparison to GPB. Thin and

permeable nature of cell wall might have permitted the easy shuttling of redox mediators (MET) aiding for efficient electron transfer in BEC_P in comparison to BEC_{P+B} and BEC_B attributing to the significant role of GNB as electrochemically active bacteria.

Keywords: Bacteria cell wall; Direct electron transfer (DET); Mediated electron transfer (MET); Membrane proteins; Microbial fuel cell (MFC).

1. Introduction

Electron transfer (ET) from bacteria to electrode is considered to be crucial for power production in bio-electrochemical (microbial fuel) cells (BEC)[1-3]. The potential created at anode by the biocatalyst influences the electron discharging capacity[4-6]. Electron transfer from the bacteria towards electrode can be distinguished as direct mode (direct electron transfer (DET)) by membrane bound proteins or by the formation of biofilm and mediated mode (mediated electron transfer (MET)) where mediators such as thionine, methyl viologen, humic acid, etc. play a key role. Bacteria catalyze the degradation of carbon sources by diverse anaerobic metabolic pathways in BECs to generate intracellular electrons, which are subsequently transferred to electrodes via DET by redox C-type cytochrome on the membrane/conductive pili/biofilm or/and MET by electron shuttles. The electron shuttle mediated ET is the widely used electron transfer pathway in most of the electrochemically active bacteria such as *Shewanella sp., Aeromonas sp.*, etc. Bacterial outer membrane is often less permeable for the transport of electro shuttles across the cell membrane which limits the electron transfer and power output of a BEC.

Physical and chemical aspects of the bacterial cell structure/wall including its permeability have regulating influence on the electron shuttle mediated extra cellular electron transfer (EET), which obviously have significance with the bioelectrogenic activity/power output. The electron transfer mechanism was specific and unlike in gram positive (GPB) and gram negative bacteria (GNB). The disparity in electron transfer between both these bacteria originates from the cell structure and composition which limits the whole scheme of electron delivery. Electrogenic capabilities of GPB and GNB differ significantly and the bacteria capabilities for bioelectricity generation were evaluated either individually or by bioaugmentation studies[7].GNB mono-

cultures such as *Pseudomonas aeruginosa*[8], *Shewanella putrefaciens*[9], *Shewanella oneidensis*[10,11], *Shewanella haliotis*[12], *Escherichia coli*[4] and *Rhodoferaxferrireducens*[13] were evaluated in various biofuel cell operations. *Pseudomonas, Shewanella and Geobacter* related to GNB were reported to have good electrogenic activity. Similarly, there have been studies on GPB such as *Brevibacillus sp*. PTH1[14], *Clostridium acetobutylicum, clostridium thermohydrosulfuricum*[15,16]*, Arthrobacterpolychromogenes* and *Corynebacterium glutamicum*[7]. The average power densities of GNB and GPB were reported to be 33 mW/m^2 (*Psuedomonas aeruginosa*)[17] and 7.3 mW/m^2 (*Corynebacterium sp.* [18]), respectively (operated under diverse conditions).

It can be presumed that the cell wall composition and structural differences of GPB and GNB may affect their growth rates and electron transferring (delivering) properties. The cell wall of GPB is generally thick which composes of 90% peptidoglycan and 10% techoic acid. Techoic acid enables the organism to adhere to the substratum (usually electrode surface) and contributes to the formation of biofilm thereby allowing electron transfer[6]. However, mechanisms of microbial electron transfer to solid electrode surfaces are not well defined in most electrochemically-active microorganisms, particularly in GPB[19]. On the contrary, the cell wall of GNB is relatively thin, porous (due to presence of porins) and lacks techoic acid. GNB has an outer membrane which is composed of thin layers of peptidoglycan that is selectively permeable to ions/metabolites etc secreted during the metabolism. The actual electron transfer mechanisms were observed to vary in each species of GNB depending on the nature and type of secretion during their metabolism. However, the exact mechanism of disparity in electron transfer between GPB and GNB under similar conditions is not reported so far. Hence, the current study is aimed

to understand the electron discharge/transfer and losses between GPB and GNB under bio-electrocatalyzed microenvironment in a defined bio-electrochemical cell. *Bacillus subtilis*, GPB and *Psuedomonas otitidis,* GNB were chosen as biocatalysts in the study to understand the underlying ET mechanisms with respect to the difference in cellular structure and composition. Thus, experiments were designed and performed using a GPB and GNB since they were considered to be electrochemically active during bio-electrochemical cell operations along with the combination of both bacteria in three individual bio-electrochemical cells.

2. Materials and Methods

2.1 Biocatalyst

Facultative anaerobic cultures from the long term operated biohydrogen reactors and aerobic sludge from poly hydroxyalkonates (PHA) producing reactor were enriched in specific medium and the individual colonies were isolated based on the morphology with repeated streaking techniques. Genomic DNA from the pure isolates was extracted using phenol chloroform method as described earlier[20]. 16S rRNA gene was amplified by PCR (Eppendorf) using purified DNA as template using universal 16S rRNA primers (Forward AF 5'-AGA GTT TGA TCC TGG CTC AG-3' (target 8-28), Reverse CR 5'-AAG GAG GTG ATC CAG CCG CA-3' (target 1542-1522))[21]. PCR amplification was programmed for an initial denaturation at 96^{o} C for 5 min, 35 cycles of denaturation (40 s at 94^{o} C), annealing (50 s at 52.6^{o} C) and extension (1 min at 72^{o} C) followed by a final extension (72^{o} C for 8 min). Amplified PCR products were sent to MWG Biotech for sequencing analysis. Both the 16S rDNA partial sequences were identified as *Pseudomonas otitidis* (accession number: HE612874) and *Bacillus subtilis* (accession number: FR849706) using the BLASTN facility (http://www.ncbi.nlm. nih.gov/BLAST/) that showed

more than 97% sequence similarity with the nearest phylogenetic neighbours, and the respective strains were used as biocatalysts in the operation of bio-electrochemical cells.

2.2 Bio-electrochemical cell

Three single chambered bio-electrochemical cells (BEC) were designed and fabricated in the laboratory using "perspex" material with a total/working volume of 0.50/0.45 l. Non-catalyzed graphite plates (5 x 5 cm; 10 mm thick) with surface area of 70 cm^2 were used as electrodes. The anode was completely immersed in the anolyte (nutrient media containing pure culture), while the upper portion of the cathode was exposed to air (open-air cathode) and the lower half portion was in contact with the anolyte. Proton exchange membrane (PEM; Nafion117, Sigma-Aldrich) was sandwiched between the electrodes to allow the exclusive transfer of protons. The upper portion of the anode was fixed below the PEM-cathode assembly over the liquid layer and the bottom surface was in contact with the anolyte. Provisions were made in the design for sampling, wire input, inlet and outlet ports. Copper wires sealed with an epoxy sealant were used to maintain contact with the electrodes and were used as current collectors. Leak proof sealing was employed to maintain anaerobic microenvironment in the system. The bio-electrochemical cells were sterilized in autoclave (15 min; 121^o C) prior to operation. Experiments were carried out without addition of any external mediators.

2.3 Experimental methodology

Prior to inoculation, the biocatalysts were re-suspended in sterilized (15 min; 121^{o}C) designed synthetic wastewater (DSW; acetate 3 g/l; NH_4Cl 0.5 g/l, KH_2PO_4 0.25 g/l, K_2HPO_4 0.25 g/l, $MgCl_2$ 0.3 g/l, $CoCl_2$ 25 mg/l, $ZnCl_2$ 11.5 mg/l, $CuCl_2$ 10.5 mg/l, $CaCl_2$ 5 mg/l, $MnCl_2$ 15 mg/l, $NiSO_4$ 0.16 g/l, $FeCl_3$ 0.03 g/l) for 12 h at room temperature. The resulting pellets of *P. otitidis,*

(BEC$_P$), *B.subtilis* (BEC$_B$) and combination of both the strains (BEC$_{P+B}$) were inoculated individually into each of the three BECs, respectively and were operated for six cycles each with a retention period of 48 h. All the three systems were operated under similar conditions and feed replacement was done with sterilized DSW at an organic load of 3 g COD/l. Prior to loading, pH of the DSW was adjusted to 6 using 2 N ortho phosphoric acid or 1 M NaOH. Constant voltage outputs and substrate (COD) removal efficiency were considered as indicators to assess the stabilized performance of the bio electrochemical cell and all the experimental operations were carried out in fed-batch mode. Before every feeding event, the inoculum was allowed to settle down (30 min; settling) and the exhausted feed was decanted (15 min; decanting). The inoculum settled at the bottom was used for subsequent operations. Feeding, decanting and recirculation operations were performed using peristaltic pumps and the operation was properly carried out to ensure that sterile microenvironment is maintained. All the experiments were performed at ambient temperatures (29±2^oC) and the anode chamber was sparged with oxygen free N_2 gas after inoculation and after every feeding event for a period of 2 min to create anaerobic microenvironment.

2.4 Process Monitoring

The performance of BEC$_P$, BEC$_B$ and BEC$_{P+B}$ was evaluated on the basis of their behavior in terms of open circuit voltage (OCV), substrate degradation and current generation patterns. Bio-electrochemical cell behavior was assessed by performing polarization with the function of current density against potential and power density measured at different resistances (30–0.05 kΩ). Anode potentials were also measured at variable external resistances to find the sustainable power generation. Cyclic voltammetry (CV) was employed to evaluate the electron discharge properties of the biocatalyst, using a potentiostat–galvanostat system (PGSTAT12, Ecochemie).

CV was operated by applying a potential ramp to the working electrode (anode), at a scan rate of 30 mV/s over a range of + 0.5 to - 0.5 V. Electron transfer rate (K_{app}) was derived by recording CV at variable scan rates. All the bio-electrochemical assays were performed *in situ*, by considering the anode and cathode as working and counter electrodes, respectively, against an Ag/AgCl (S) reference electrode. Tafel analysis was made from the voltammetric profiles using GPES (version 4.0) software and conclusions were drawn in terms of Tafel slopes and polarization resistance. Volatile fatty acids (VFA), pH and chemical oxygen demand (COD) were evaluated based on the procedures depicted in the standard methods[22]. High performance liquid chromatography (HPLC; Shimadzu LC10A) was employed to quantify the VFA with UV-Vis detector at 210 nm and C18 reverse phase column (250 x 4.6 mm dia particle size) using 40% acetonitrile in 1 N H_2SO_4 (pH, 2.5-3.0) as mobile phase with a flow rate of 0.5 ml/min.

3. Results and discussion

3.1 Bio-electrogenic activity

After inoculating the three individual BEC's with GNB (*P. otitidis),* GPB *(B. subtilis)* and combination of both (GNB+GPB), bio-electrogenic activity was monitored in terms of open circuit voltage (OCV) and current (Fig. 1). During the initial cycles of operation, BEC_{P+B} (combination of both GPB and GNB) showed relatively higher OCV and current (160 mV; 1.23 mA) than BEC_P (148 mV; 1.12 mA) and BEC_B (135 mV; 0.93mA). During the course of operation, BEC_P (338 mV; 1.42 mA) and BEC_{P+B} (318 mV; 1.21 mA) showed more or less similar performance, whereas, BEC_B (242 mV; 1 mA) showed the least electrogenic activity. By the end of operation, BEC_P (371 mV; 1.67 mA) documented highest electrogenic activity followed by BEC_{P+B} (336 mV; 1.24 mA) and BEC_B (268 mV; 1.20 mA). Although higher

electrogenic activity was observed with BEC_{P+B} in the initial cycles of operation, BEC_P gradually attained the highest power output by the end of the cycle operation. The observed difference documents the electrogenic capabilities of GNB in terms effective EET mediated through the redox shuttles. Though there was an association of both the strains in the third BEC, higher electrogenic activity over BEC_P was not observed which might be attributed to the higher electrochemical activity of GNB in comparison to the dual association of both the bacteria. Also, there might have been a syntrophic association between GPB and GNB where GNB might have utilized the electrons discharged from GPB towards its growth and metabolism that ultimately contributes for higher electrogenic activity.

Fig 1

3.2 Electron transfer

The bio-electro catalytic behavior of biocatalyst in terms of electron discharge (ED), redox catalytic currents, electron transfer to anode, electron neutralization at cathode, capacitance, charge, energy and substrate oxidation can be determined from CV analysis[23]. The bio-electrocatalysis of anode controls the energy conversion efficiency which is significantly related to the electron transfer scheme between the microbes and electrode[24]. CV helps to characterize the electron transfer interactions between microorganisms or microbial metabolites by applying an external potential[25]. Voltammograms (vs Ag/AgCl (S)) measured *in situ* through CV visualized marked variation in the ED properties and energy generation pattern with the function of nature of biocatalyst (Fig. 2). BEC_P recorded higher redox catalytic currents compared to BEC_B and BEC_{P+B} during forward and reverse sweeps. In the case of BEC_P, reduction currents (RC) were significantly higher than the oxidation currents (OC) which were more or less similar

(RC: -10 mA and OC: 25 mA) during all the time intervals except at 24th and 36th h. The OC and RC were distinctively higher during 24 h (RC, -50 mA; OC, 40 mA) depicting higher electrogenic activity that aids in effective discharge and transfer of the redox equivalents as well as their reduction at a higher rate. The redox currents were found to decrease gradually from 24th to 36th h and rapidly from 36th h till the end of operation depicting the stationary phase followed by a decline phase in the growth cycle of bacteria. *P. otitidis,* GNB is capable of discharging/transferring electrons through mediated electron transfer (MET) due to the permeable nature of cell wall that allows easy diffusion of redox equivalents thus contributing for higher power output. The redox shuttles as electron carriers would have minimized the electron losses, contributing for an increment in the electrogenic activity.

BEC_B and BEC_{P+B} recorded lower catalytic currents compared to BEC_P. However, BEC_{P+B} showed marginally higher currents in comparison to BEC_B. In the case of direct electron transfer (DET), EET takes place through the biofilm (electrochemically active bacteria adhere to the substratum due to exo-polysaccharides and lipotechoic acid), membrane bound proteins or nano wires to the electrode surface[6,26]. The redox catalytic currents in both the BECs were more or less similar (BEC_B: OC: 10±5 mA; RC -15±10 mA and BEC_{P+B}: OC: 15±10 mA; RC: -5±10 mA) till 18th h of operation. An increment in currents was observed during 24th h of operation attributing to the rapid electron transfer. Also rapid substrate degradation due to higher metabolic activities of the biocatalyst result in efficient ED. OC (BEC_B: 30 mA; BEC_{P+B}: 30 mA) was slightly higher in comparison to RC (BEC_B: -25 mA; BEC_{P+B}:-30 mA) during 24th h. Later, a decrement in OC and an increment in RC was observed during 36th h (OC: 15±5 mA; RC: -30±5 mA) which continued till the end of operation (OC: 5±15 mA; RC: -30±5 mA) in both the BECs. The decrement in oxidation reactions can be attributed to substrate exhaustion or the losses

during electron transfer in the anode chamber, while an increment in reduction currents might be due to effective neutralization capabilities of the biocatalyst as well as the reduction of the accumulated metabolic intermediates. The extent of biofilm growth and its coverage on the anodic surface has direct influence on both power production and substrate degradation[23].The self-immobilized biofilm on the anode surface shows effective power generation potential indicating direct extracellular electron transfer in the absence of soluble mediator. However, the increase in thickness of biofilm beyond the optimum level hinders the electron transfer due to the resistance offered by biofilm. The observed higher redox currents in BEC_P in comparison to BEC_B and BEC_{P+B} highlights the role of redox shuttles as electron carriers in GNB, which increase the ET efficiency over GPB.

Fig. 2

The first derivative of CV (DCV) helps to study the EET site of a redox species involved during the electron transfer on the redox voltammetric signature[27]. DCV analysis also facilitates the interpretation of the rate of change in voltammetric current (i) with respect to the electrode potential E (di/dt).During DCV analysis, three quasi reversible peaks were detected in BEC_B at EET sites with peak potentials of 0.04 V, 0.211 V and 0.423 V corresponding to the involvement of redox species (RS) viz., cytochrome bc1, cytochrome-C and cytochrome aa3, respectively (Fig. 3). These membrane bound proteins are organized components (either tightly bound or soluble) that aid in the ET process of bacteria through DET mechanism, specifically with GPB. In the case of *P. otitidis*, two quasi reversible peaks were detected at potential of -0.036 V and -0.176 V which relates to phenazine derivative and Fe-S proteins, respectively mediating the ET. *Pseudomonas* is capable of secreting redox mediators that aids in electron transfer[28]. The observed peak potential (-36 mV) might correspond to the redox potential of the *Pseudomonas*

phenazine derivatives. Phenazines are signaling molecules in *Pseudomonas. sp*, which can facilitate the communication through quorum sensing (QS) mechanism in the biofilm apart from enhancing the production of extracellular polysaccharides[17,29] . These molecules act as redox mediators after they are released into the anolyte[30]. These phenazine redox mediators are detected at negative potential (peak at -36 mV in first DCV) which tends to have more affinity as an electron carrier. They also act as reducing agent and can donate electron to the highly potential/positive potential compound (electrode or substrate). The observed phenazine derivative elucidates the specific role of QS in aiding electron transfer[31] through MET mode which resulted in enhanced power generation. Similarly, the redox mediators for GPB (cytochromes) detected at positive redox potential will have relatively less electron affinity in comparison to GNB. The increment in power output as well as the higher electrogenic activity with GNB than GPB illustrates the exogenous shuttling activity through the redox metabolites (detected at negative potentials) secreted by *P. otitidis*. However, no specific peaks were detected for BEC_{P+B} in the study.

Fig. 3

3.3 Bio-electrokinetics

BEC operations undergo many electron losses during the transfer of electrons from the biocatalyst to anode which lowers the conversion efficiency. Especially at lower current densities, activation losses are considered to be crucial[32]. The redox equivalents generated during substrate metabolism need to overcome many barriers prior to reaching anode and then cathode. During this process, there exist many possibilities of electron losses either due to neutralization or the acceptance by other electron acceptors, which can be termed as electron quenching[33].

Hence, biocatalyst, BEC operation and the factors that govern the operation play a crucial role in the effective transfer of electrons. The efficiency in higher power generation or minimization of losses is directly proportional to the aforementioned factors. Electron losses can be understood through polarization curve as well as by Tafel analysis which derives the active kinetic parameters[23]. The bio-electrokinetics of biocatalyst in terms of electron transfer rate was calculated as K_{app} which gives the number of electrons transferred per second to the electrode[34].

3.3.1 Electron losses-Influence of external load

The electron discharge (ED) pattern of GPB and GNB with respect to the external resistance was well illustrated by performing polarization across a wide range of resistances (30 KΩ to 100 Ω). Current through the circuit was observed to increase with the decrease in external load reaching cell design point (CDP), where ED was higher in terms of power. At higher resistances, the current observed was negligible in all the BECs suggesting the non-responsive nature of the biocatalyst to higher loads. Generally activation, ohmic and concentration losses will be encountered during BEC operation. Polarization profiles of the GPB and GNB illustrate a clear variation in the CDP where the BECs can be operated (Fig. 4). BEC_P attained highest CDP (280 Ω) with a power density of 63.3 mW/m^2 followed by BEC_{P+B} (CDP: 270 Ω; PD: 47.7 mW/m^2) and BEC_B (CDP: 220 Ω; PD: 35.5 mW/m^2). Relatively high potential drop was observed at low resistances which might be attributed to the effective ED observed. Activation and concentration losses were found to be observed during the operation of the three BECs. The higher CDP of *P. otitidis* indicates the ability of GNB towards higher electrogenic activity and also reflects the stabilized performance at higher resistances inferring the elimination of activation losses. BEC_{P+B} attained a slightly lesser CDP next to BEC_P indicating the positive influence of synergistic association between the two cultures due to MET than DET attributing the feasibility

of endogenous redox shuttles participating in the ET in comparison to the membrane bound proteins. Lower electrogenic activity observed with BEC_B also infers the occurrence of concentration losses due to the less efficiency in ET in comparison to the redox shuttles that would minimize the losses. Lower CDP along with low ED is proportional to the activation losses encountered during operation in transferring the electrons from the inner bacterial membrane to the external environment.

Fig. 4

3.3.2 Tafel analysis

The redox slopes as well as the shifts in Tafel plots provide a clear understanding of the electron losses. Higher oxidation slope indicates the requirement of higher activation energy that makes oxidation less favorable. Conversely, lower oxidation slopes indicates the requirement of lower activation energy that makes oxidation more favorable. The same can be related in case of reduction slope as well as polarization resistance (R_P). Reduction reactions were found to be dominant over oxidation reactions during the operation of three BECs (Fig. 5a). Initially all the systems showed lower redox slopes (ba: 0.30±0.39 V/dec; bc: 0.05±0.25 V/dec) which then increased (ba: 0.35±0.47 V/dec; bc: 0.05±0.19 V/dec) by the end of operation. This trend corresponds to the availability of good amount of substrate during initial hours for the rapid metabolic activities of bacteria and the increment in slope corresponds to the electron losses (concentration losses). In the case of oxidation slope for all the three BECs, an immediate increment (0.65±0.14 V/dec) was observed after the initial hours (0.32±0.39 V/dec), which can be ascribed to the activation losses that require energy to cross the barriers for ET towards working electrode. During the course of time (18-36 h), ET was found to be efficient due to the

decrement in losses either due to the participation of soluble redox shuttles or the membrane associated cytochromes. The reduction reactions that were dominant during the BEC operation were wavering in the case of BEC_P and BEC_B, while a continuous increment was observed in the case of BEC_{P+B}. However, higher reduction (lower slope) was observed in BEC_B (0.054 V/dec) followed by BEC_P (0.108 V/dec) and BEC_{P+B} (0.219 V/dec). The observed pattern corresponds to the ability of *B. subtilis*, in reducing the redox equivalents effectively for the formation of metabolic end products. The continuous increment of reduction slopes observed in the case of BEC_{P+B} might be due to the prevailing concentration losses in the BEC system.

Fig.5a

The shifts in Tafel plots also provide a visual understanding of the typical behavioral changes of the BECs towards reduction (-0.4 V) providing more number of protons during the course of operation[33]. BEC_P and BEC_{P+B} showed the behavioral shift from the mid-point potential (0 V) towards reduction, whereas, BEC_B remained at reduction (negative potentials) and showed a slow shift towards mid-point/oxidation at the end of operation (48 h) (Fig. 5b).The shift towards reduction elucidates the higher neutralization or reduction capabilities of biocatalyst that enhance the power generation performance as the reduction at cathode limits the whole performance of BEC. Also, a shift towards oxidation explains the higher substrate degradation capabilities of bacteria that subsequently release the reducing equivalents (e^- and H^+) which are the redox powers for the bioelectrogenic activity. The shift exhibited by *B. subtilis* towards oxidation is in accordance with the observed substrate degradation capabilities which are relatively higher over BEC_{P+B}. Though, marked shifts that are good indicators of the redox behavior of biocatalyst noticed during the operation, the electron losses that are encountered during the operation seems to limit the whole power output of a BEC.

Fig. 5b

3.3.2.1 Resistance to electron transfer

The resistance for electron transfer either from the biocatalyst to anode or from the anode to cathode is termed as polarization resistance (R_P), which hampers the electron flow during the operation. Higher R_P was observed with BEC_B followed by BEC_{P+B} and BEC_P (Fig. 6). GPB has a general tendency of forming a biofilm on the electrode surface that will enable the transfer of electrons from the bacterial cell towards the electrode in another way acting as an electron donor[35]. Also, higher deposition of biofilm (more thickness) does not permit the efficient electron transfer[36]. *B. subtilis* being a GPB could form a biofilm and confer to the attached growth due to the presence of lipotechoic acid in the cell wall depicted higher R_p (198 KΩ) during the BEC operation. Also, the interaction of GPB and GNB in BEC_{P+B} could not contribute for significant electron delivery and showed 128 KΩ resistance which is comparatively higher than *P. otitidis* (93.8 KΩ). The higher resistance in BEC_{P+B} than BEC_P might also have resulted in electron losses during the operation of both the strains. However, low R_P observed with GNB supports the efficient electron transfer (which was also aided by redox shuttles) signifying the lowered electron losses.

Fig. 6

3.3.3 Electron transfer rate

The bio-electro kinetics of biocatalyst during the BEC operation was derived from CV recorded under varying scan rates. It helps to analyze the dependency of the peak currents and to deliberate the electron transfer rates based on the bio-electrochemical reversibility. The

dependence of peak potential on the scan rate (mV/s) was evaluated when $\Delta E_p \geq 200$ mV ($\Delta Ep = E_{pc} - E_{pa}$) where E_{pc} and E_{pa} represents cathodic and anodic peak potential, respectively[37].

$$E_{pc} = E^0_c - [RT/\alpha nF] \ln [\alpha nF\nu_c/RTk_{app}] \quad \ldots\ldots\ldots (1)$$

$$E_{pa} = E^0_a - [RT/(1-\alpha)nF] \ln [(1-\alpha)nF\nu_a/RTk_{app}] \quad \ldots\ldots\ldots (2)$$

Variation in the electron transfer rate was observed with the function of biocatalyst and operation time (Fig.7). The rate of ET can be influenced by the applied voltage and thebehavior can be quantified using the K_{app} model. Based on the variation in sweep rate, electron transfer rates between the biocatalyst and the electrodes were calculated as electron transfer rate constants (K_{app}), which provide a direct approach to quantitatively compare the electrochemical activity of the biocatalysts. The k_{app} value was calculated for BEC_P, BEC_{P+B} and BEC_B, respectively by substituting the slopes obtained from the voltammograms in the above two equations. At higher scan rates, the redox peak potential (E_p) followed increasing trend which might be due to development of ohmic potential during BEC operation[38]. Higher K_{app} was observed with BEC_P (81 s^{-1}) followed by BEC_{P+B} (67 s^{-1}) and BEC_B (53 s^{-1}) which elucidates the fast and quick electron transfer capabilities of GNB in comparison to GPB. Relatively higher K_{app} value of BEC_P over BEC_B in the present study elucidates the electrochemically active shuttling nature of GNB that exhibit MET through phenazine redox shuttles, which facilitate easy and fast electron diffusion of electrons. Similarly, low K_{app} observed with GPB might be due to the slow rate of electron diffusion through membrane bound proteins that lack the shuttling activity.

Fig.7

3.4 Relative decrement in anode potential (RDAP)

The relative decrement in anode potential (RDAP) with the function of applied external resistance was used to evaluate the maximum sustainable power/sustainable anodic resistance of the BECs. The BEC will be in steady state if the power generated by the system equals the power consumption for an extended time. Figure 8depicts the variation of percent deviation of anodic potential with respect to applied external resistance. High external resistance limits the electron delivery to the cathode, while at lower external resistance, the electron delivery to the cathode is limited by kinetic and /or mass transfer (or internal resistance)[39]. Electron-transferring system of microbes generally lies at a level just below the anode potential[40]. Moreover, anode potential controls the kinetics of electron transfer from the microorganism to the anode. Anodic oxidation potential also determines the theoretical energy gain of the biocatalyst from a thermodynamic point of view, irrespective of the metabolic pathway it undergoes. Lower oxidation potential at anode provides less energy for the growth and maintenance of the biocatalyst, while higher oxidation potential supports early start up of the ED and on a whole higher current generation. The maximum sustainable resistance was higher for BEC_P (5 kΩ) which is more or less equal to BEC_{P+B} (4.8 kΩ). While in the case of $BEC_{B,}$ the sustainable resistance (4.5 kΩ) was slightly less in comparison to the other two BECs. This shows the potential of GNB in effective ED against higher resistance over GPB. The concentration losses as well as the activation losses were found to be slightly for GNB in comparison to GPB depicting the efficiency of electron discharge capabilities of *P. otitidis.*

Fig. 8

3.5 Sustainable current

Chronoamperometry (CA) enumerates the maximum feasible sustainable current. Initially, maximum current generation will be observed and with the time, current decreases and stabilizes at certain point which can be considered as sustainable current[37]. CA were recorded by applying a constant potential of 0.5 V. Cellular growth, metabolism and enzymatic processes can be influenced or driven by electrons donated from electrodes to microorganisms by multiple approaches viz., applied potential experiments[41]. After maximum current density was reached, a period of stable current production was observed[42]. BEC_P initially showed higher currents (40 mA) which then documented a steep drop to 6 mA and showed sustainable current generation (5 mA) for 900 sec. Initially BEC_B and BEC_{P+B} showed 13 mA and 3 mA currents which again dropped to 6 mA and 2 mA, respectively. Thereafter, stabilized currents of 3 mA and 1 mA were recorded for BEC_{P+B} and $BEC_{B,}$ respectively (Fig. 9). This behavior is ascribed to the higher electrogenic capabilities of GNB over GPB. The sustainable currents in BEC_{P+B} lies in between BEC_P and BEC_B generating slightly higher currents over GPB attributing to the influence of synergistic interaction.

Fig. 9

3.6 Substrate degradation

Degradation of substrate varied based on the anodic biocatalyst used in the BEC. A gradual depletion in substrate (COD concentration) was observed with operation time in all the BEC (Fig.9a). However, substrate degradation rates (SDR) and the ability in releasing the redox equivalents was observed to vary depending on the inherent capabilities of biocatalyst. Higher SDR with COD removal efficiency (COD_R) was observed for BEC_P (SDR, 1.23 kg COD/m^3-

day; COD_R: 75%) followed by BEC_B (SDR, 1.04 kg COD/m^3-day; COD_R: 62%) and BEC_{P+B} (SDR, 1.00 kg COD/ m^3-day; COD_R: 60%). Higher SDR and COD_R observed with BEC_P operation obviously supports higher bio-electrogenic activity that is in concurrence with the discharge of more number of redox equivalents. On the contrary, though BEC_B was observed to yield less current, SDR was observed to be higher in comparison to BEC_{P+B}. In BEC_{P+B} system, there might be a competition for growth of cells between *B. subtilis* and *P. otitidis* and hence would compete to utilize the substrate. Substrate degradation was more or less similar for BEC_B and BEC_{P+B} systems and based on this observation, *Bacillus. sp* appear to be dominant than *Psuedomonas. sp* in BEC_{P+B} system. Though GPB has efficiency in discharging higher number of redox equivalents, the ability of electron transfer was found to be less in comparison to GNB and hence lower currents were observed with BEC_B. Biofilm also has a significant influence on the efficiency of the substrate conversion process[43].

Fig. 10a

Volatile fatty acids (VFA) and pH are the active intrinsic expressers of acid and base reactions of the system. Inlet pH of all the BECs was adjusted to 6 and a consistent drop in pH (5.4±0.3) was observed in all the systems throughout the operation (Fig. 9b). Drop in pH was associated with simultaneous generation of VFA. Higher VFA generation was observed in BEC_B (1148 mg/l) followed by BEC_{P+B} (1020 mg/l) and BEC_P (998 mg/l).pH values correlate well with the corresponding VFA concentration. The acid metabolites formed were composed of formic acid, acetic acid and butyric acid for BEC_P, BEC_B and BEC_{P+B}, respectively.

Fig. 10b

4. Conclusions

The present study illustrates the variation in electron transfer capabilities of GPB and GNB and combination of both in a defined BEC operated at similar conditions. Higher electrogenic activity by GNB over GPB is due to the role of redox shuttles as electron carriers that mediate the electron transfer which are detected as peaks/EET sites (phenazines detected at negative potentials) during DCV analysis. GPB exhibited DET through the membrane bound proteins (cytochromes detected at positive potentials) that could transfer electrons at a lesser rate than mediated mode contributing for lower power output, compared to GNB. In addition, the EET sites that are detected at negative potential have relatively higher electron affinity either to accept/release than the EET sites at more positive potential during the redox reactions. This is in concurrence with the high electrochemical activity of GNB that exhibited MET through the redox shuttles detected at negative potentials. Though there was an association of both the strains in BEC_{P+B}, much improvement in electron transfer was not observed attributing to the minimal influence of dual strain interaction. BEC_P showed relatively higher redox currents, K_{app} along with lower Tafel slopes and polarization resistance compared to BEC_{P+B} and BEC_B. Structural differences (presence of permeable and thin cell wall in GNB than GPB) among the bacteria also resulted in lowered electron losses and made the diffusion of electron shuttles more feasible in GNB, contributing for higher electrogenesis. Further, comprehensive studies based on the cell structure employing diverse GNB and GPB strains will help to shed more light on the electron flux aspects in bio-electrogenic environment.

Acknowledgements

The authors wish to thank the Director, CSIR-IICT, Hyderabad for support and encouragement in carrying out this work. Authors duly acknowledge Department of Biotechnology (DBT), Government of India for providing research grant in the framework of National Bioscience Award 2012 (BT/HRD/NBA/34/01/2012(vi)). Part of the reported research was supported by CSIR-XII five year network projects (SETCA, CSC-0113). JAM would like to acknowledge the fellow colleagues R.K.Goud and M.V.Reddy for providing *P. ottitidis* and *B. subtilis* strains to carry out the work.

References

1. B. E. Logan, S. Cheng, V. Watson and G. Estadt, *Environ. Sci. Technol.* 2007, 41, 3341-3346.

2. J.Y. Nam, H.W. Kim, K.H. Lim and H.S. Shin, *Environ. Eng. Res*. 2010, 15, 071.

3. M. Rosenbaum, U. Schroder, F. Scholz, *J. Solid State Electrochem*. 2006, 10, 872.

4. U. Schroder, J. Nieben, F. Scholz, *Chem. Int. Ed. Engl*. 2003, 42, 2880-2883.

5. S.V. Raghavulu, P.N. Sarma and S. Venkata Mohan, *J. Appl. Microbiol.* 2010, 1364-5072.

6. P. S. Bonanni, G. D. Schrott, L. Robuschi and J. P. Busalmen, *Energy Environ. Sci.* 2012, 5, 6188-6195.

7. D. F. Juang and L. J. Chiou, *Int. J. Environ. Sci. Tech.* 2007, 4, 119-125.

8. K. Rabaey, N. Boon, S. D. Siciliano, M. Verhaege and W. Verstraete, *Appl. Environ. Microbiol.* 2004, 70, 5373–5382.

9. H. J. Kim, H. S. Park, M. S. Hyun, I. S. Chang, M. Kim and B. H. Kim, *Enzyme Microb. Technol.* 2002, 30, 145-152.

10. J. C. Biffinger, R. Ray, B. J. Little, L. A. Fitzgerald, M. Ribbens, S. E. Finkel, B. R. Ringeisen, *Biotech. Bioeng.* 2009, 103, 3.

11. V. J. Watson and B. E. Logan, *Biotech. Bioeng.* 2010, 105, 489-498.

12. S. V. Raghavulu, P. S. Babu, R. K. Goud, G. V. Subhash, S. Srikanth and S. Venkata Mohan, *RSC Adv.* 2012, 2, 677–688.

13. S. K. Chaudhuri and D. R. Lovley, *Nat. Biotechnol.* 2003, 21, 1229-1232.

14. T.H. Pham, N. Boon, P. Aelterman, P. Clauwaert, D. Schamphelaire, L. Vanhaecke, W. Verstraete, K. Rabaey, *Appl. Microbiol. Biotechnol.* 2008b, 77, 1119–1129.

15. A. S. Mathuriya, and V. N. Sharma, *J. Biochem. Technol.* 2009, 1, 49-52.

16. A. S. Finch, T. D. Mackie, C. J. Sund, J. J. Sumner, *Bioresour. Technol.* 2011, 102, 312-315.

17. S. V. Raghavulu, J. Annie Modestra, K. Amulya, C. Nagendranatha Reddy and S. Venkata Mohan, *Bioresour. Technol.* 2013, 146, 696–703.

18. M. Liu, Y. Yuan, L. X. Zhang, L. Zhuang and S. Z. Ni, *Bioresour. Technol.* 2010, 101, 1807–1811.

19. C. W. Marshall and H. D. May, *Energy Environ. Sci.* 2009, 2, 699-705.

20. R. K. Goud, S. V. Raghavulu, G. Mohanakrishna, K. Naresh and S. Venkata Mohan, *Int J Hydrogen Energy.* 2012, 37, 4068-4076.

21. S. Venkata Mohan, S. V. Raghavulu, R. K. Goud, S. Srikanth, V. L. Babu and P. N. Sarma, *Int J Hydrogen Energy.* 2010, 35, 12208-12215.

22. APHA, 1998. 20th edn. American Public Health Association/American water works Association/ Water environment federation, Washington DC, USA.

23. S. V. Raghavulu, S. Venkata Mohan and P. N. Sarma, *Biosens. Bioelectron.* 2008, 24, 41–47.

24. Y. Qiao, S. J. Bao and C. M. Li, *Energy Environ. Sci.* 2010, 3, 544-553.

25. R. K. Goud and S. Venkata Mohan, *RSC Adv.* 2012, 2, 6336–6353.

26. S. M. Strycharz, A. P. Malanoski, R. M. Snider, H. Yi, D. R. Lovley and L. M. Tender, *Energy Environ. Sci.* 2011, 4, 896-913.

27. X. Zhang and E. M. Marsil, *Electrochimica Acta.* 2013, 102, 252– 258.

28. T. H. Pham, N. Boon, K. D. Maeyer, M. Hofte, K. Rabaey and W. Verstraete, *Appl. Microbiol. Biotechnol.* 2008a, 80, 985–993.

29. J. D. Shrout and R. Nerenberg, *Environ. Sci. Technol.* 2012, 46, 1995–2005.

30. M. R. Parsek, and E. P. Greenberg, *PNAS. Colloquium.* 2000, 97, 8789–8793.

31. Y.C.Yong, Y.Y. Yu, C. M. Li, J. J. Zhong, H. Song, *Biosens. Bioelectron.* 2011, 30, 87–92.

32. G. Velvizhi, P. S. Babu, G. Mohanakrishna, S. Srikanth and S. Venkata Mohan, *RSC Adv.* 2012, 2, 1379–1386.

33. S. Srikanth and S. Venkata Mohan, *RSC Adv*. 2012, 2, 6576–6589.

34. E. Laviron, *J. Electroanal. Chem. Interfacial Electrochem*. 1979, 100, 263.

35. R. S. Renslow, J. T. Babauta, P. D. Majors and H. Beyenal, *Energy Environ. Sci.* 2013, 6, 595-607.

36. U. Schroder, *Phys. Chem. Chem. Phys.* 2007, 21, 2619–2629.

37. Y. Yuan, S. Zhou, N. Xu and L. Zhuang, *Colloids Surf*. 2011, 82, 641–646.

38. S. Venkata Mohan and K. Chandrasekhar, *Bioresour. Technol.* 2011, 102, 9532–9541.

39. S. V. Raghavulu, P. N. Sarma and S. Venkata Mohan, *J Appl. Microb*. 2011, 110, 666–674.

40. P. Aelterman, S. Freguia, J. Keller, W. Verstraete and K. Rabaey, *Appl. Microbiol. Biotechnol.* 2007, 78, 409–418.

41. A. W. Thomas, L. E. Garner, P. Kelly, Nevin, T. L. Woodard, A. E. Franks, D. R. Lovley, J. J. Sumner, C. J. Sundd and G. C. Bazan. 2013, DOI: 10.1039/c3ee00071k.

42. A. Alessandro, C. Martinez, M. Pierra, E. Trably, and N. Bernet, *Phys. Chem. Chem. Phys.* 2013, 15, 19699.

43. A. P. Borole, G. Reguera, B. Ringeisen, Z. W. Wang, Y. Feng and B.H. Kim, *Energy Environ. Sci.* 2011, 4, 4813-4834.

Captions for Figures

Fig.1 (a): Voltage and (b) Current generation profiles of *P. otitidis*, *B. subtilis* and P+B (combination of *P. otitidis* and *B. subtilis*) operated for a period of six cycles.

Fig.2: Cyclic voltammograms depicting the redox catalytic currents in (a) *P. otitidis*, (b) *B. subtilis, (c)* combination of *P. otitidis* and *B. subtilis* (P+B) and (d) Enhanced performance of *P. otitidis* (represented in magenta color) in comparison to *B. subtilis* (light green color) and P+B (blue color) recorded at a scan rate of 30 mV/sec.

Fig.3: First derivative of CV (DCV) derived for (a) *P. otitidis* (at -36 mV and -0.176 V) and (b) *B. subtilis* (0.04 V, 0.211 V and 0.423 V) illustrating the extracellular electron transfer (EET) site potential of redox species involved during the electron transfer.

Fig.4: Current and power density curves (polarization profile) of three systems under study measured with respect to variable external resistances (30 kΩ- 50 Ω)

Fig.5: Electro-kinetic studies represented by (a) Tafel slopes (b_a, b_c) and (b) electron transfer rates (K_{app}) recorded at variable scan rates (5 mV/sec to 150 mV/sec)

Fig. 6: Illustration of shift in redox behavior of biocatalyst operated in three systems

Fig.7: Resistance to electron transfer in terms of polarization resistance (R_P)

Fig. 8: Relative decrement in anode potential (RDAP) depicting the sustainable anodic resistance

Fig. 9: Typical chronoamperograms of BEC_P, BEC_B and BEC_{P+B} at an applied potential of 0.5 V

Fig.10: (a) COD (substrate) removal and (b) Variation in pH and VFA with respect to time in BEC_P, BEC_B and $BEC_{P+B.}$

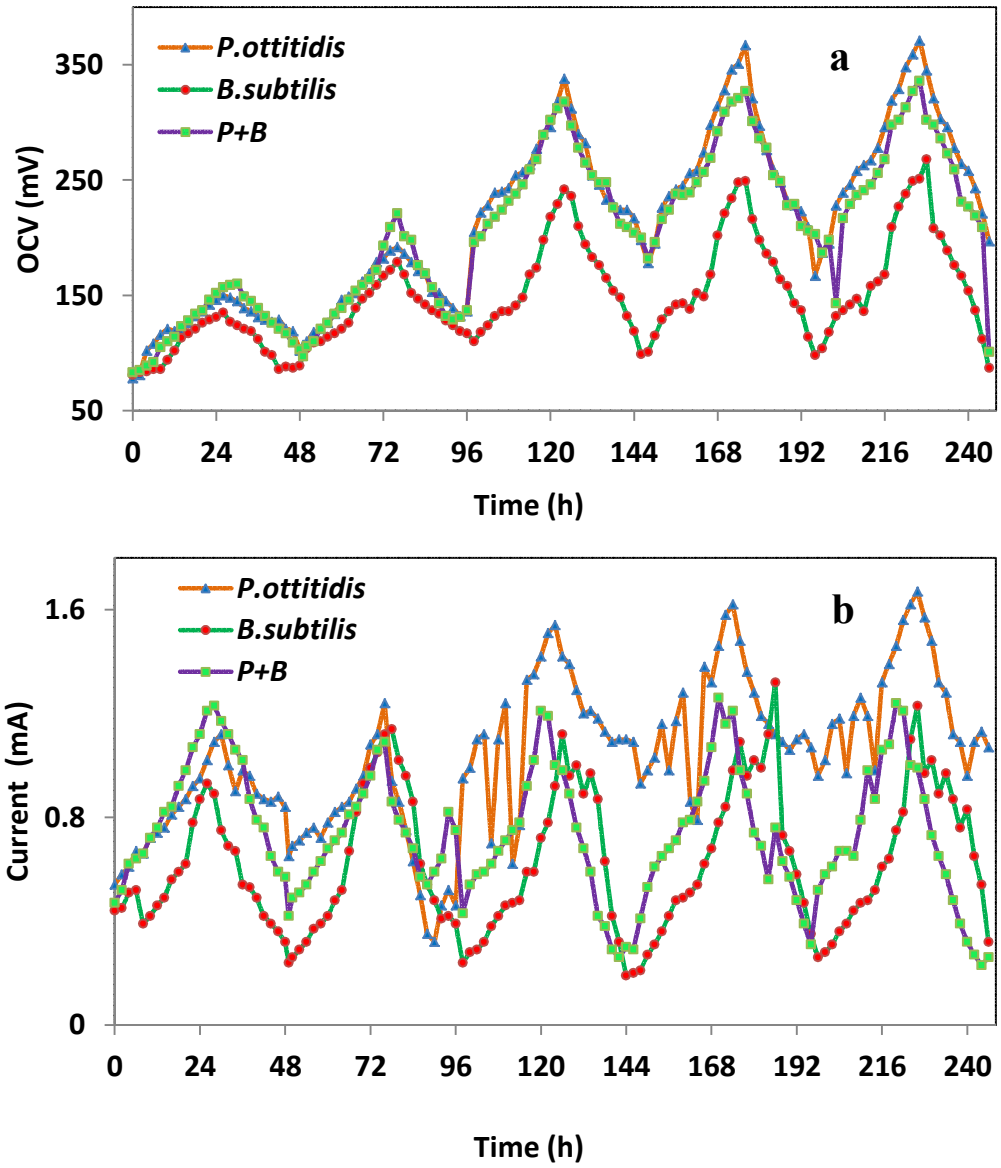
P.ottitidis
B.subtilis
P+B
a
OCV (mV)
350
250
150
50
0
24
48
72
96
120
144
168
192
216
240
Time (h)
P.ottitidis
B.subtilis
P+B
b
Current (mA)
1.6
0.8
0
0
24
48
72
96
120
144
168
192
216
240
Time (h)

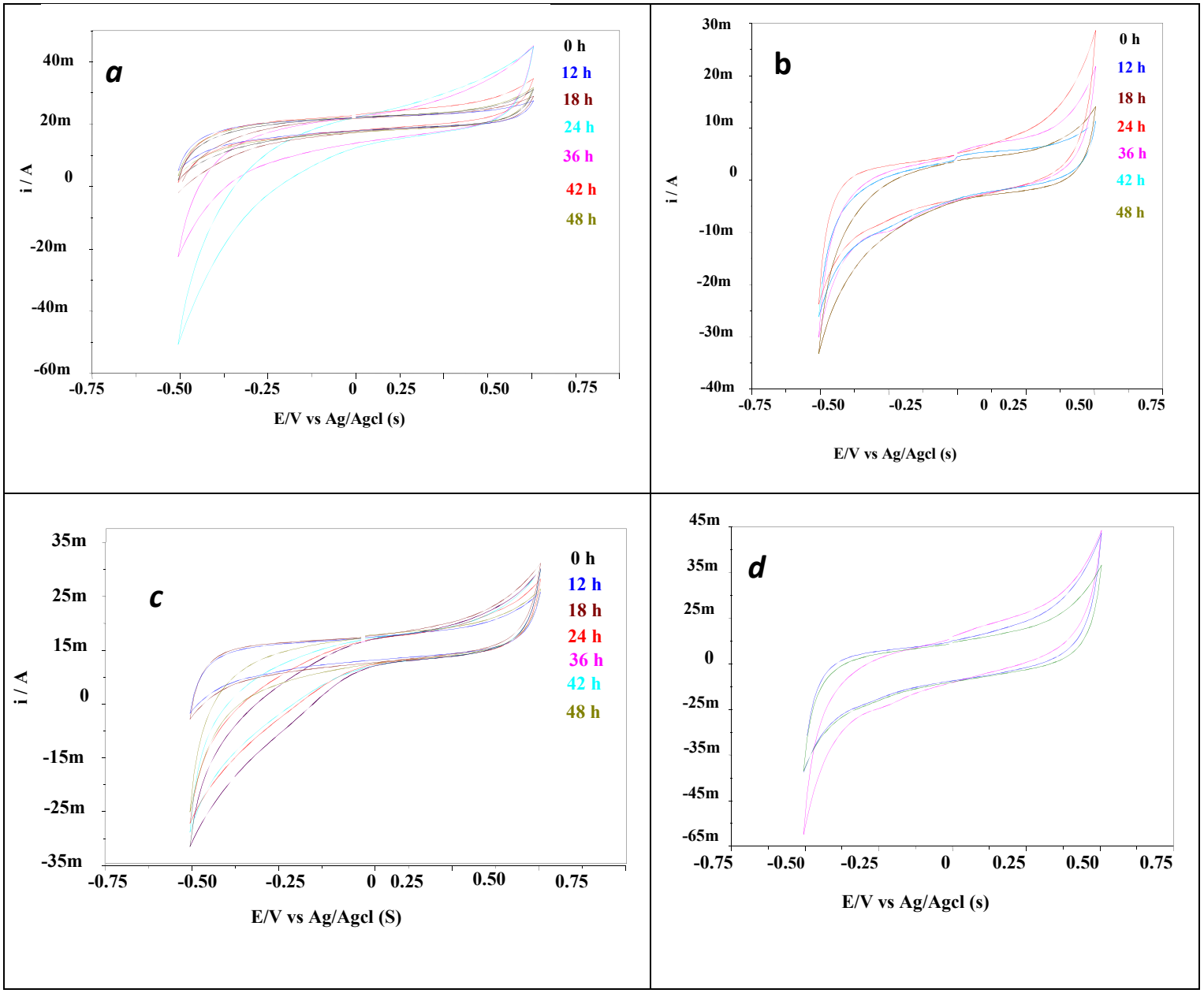
a
40m
20m
0
-20m
-40m
-60m
i / A
-0.75
-0.50
-0.25
0
0.25
0.50
0.75
E/V vs Ag/Agcl (s)
0 h
12 h
18 h
24 h
36 h
42 h
48 h
b
30m
20m
10m
0
-10m
-20m
-30m
-40m
i / A
E/V vs Ag/Agcl (s)
c
35m
25m
15m
0
-15m
-25m
-35m
i / A
E/V vs Ag/Agcl (S)
d
45m
35m
25m
0
-25m
-35m
-45m
-65m
E/V vs Ag/Agcl (s)

Fig. 2

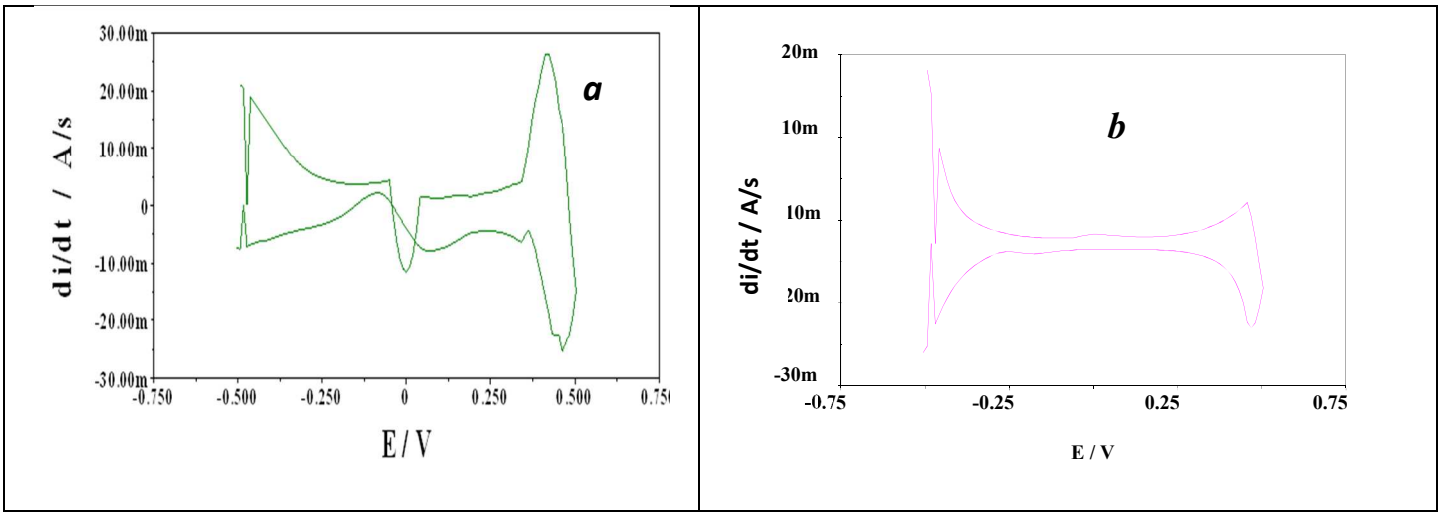
a
di/dt / A/s
E / V
b
di/dt / A/s
E / V

Fig. 3

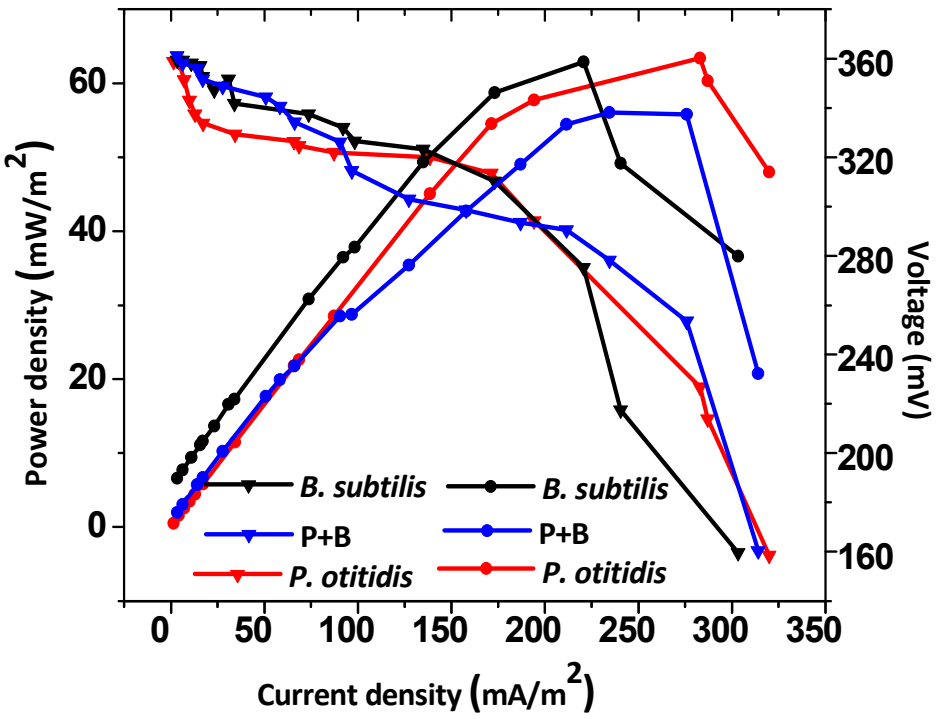
Power density (mW/m2)
Voltage (mV)
Current density (mA/m2)
B. subtilis
B. subtilis
P+B
P+B
P. otitidis
P. otitidis

Fig. 4

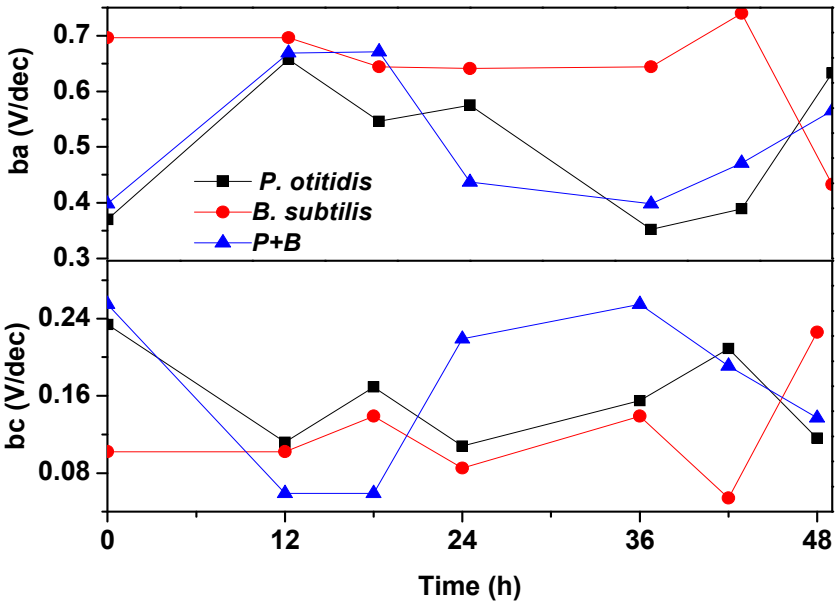
ba (V/dec)
0.7
0.6
0.5
0.4
0.3
P. otitidis
B. subtilis
P+B
bc (V/dec)
0.24
0.16
0.08
0
12
24
36
48
Time (h)

Fig. 5a

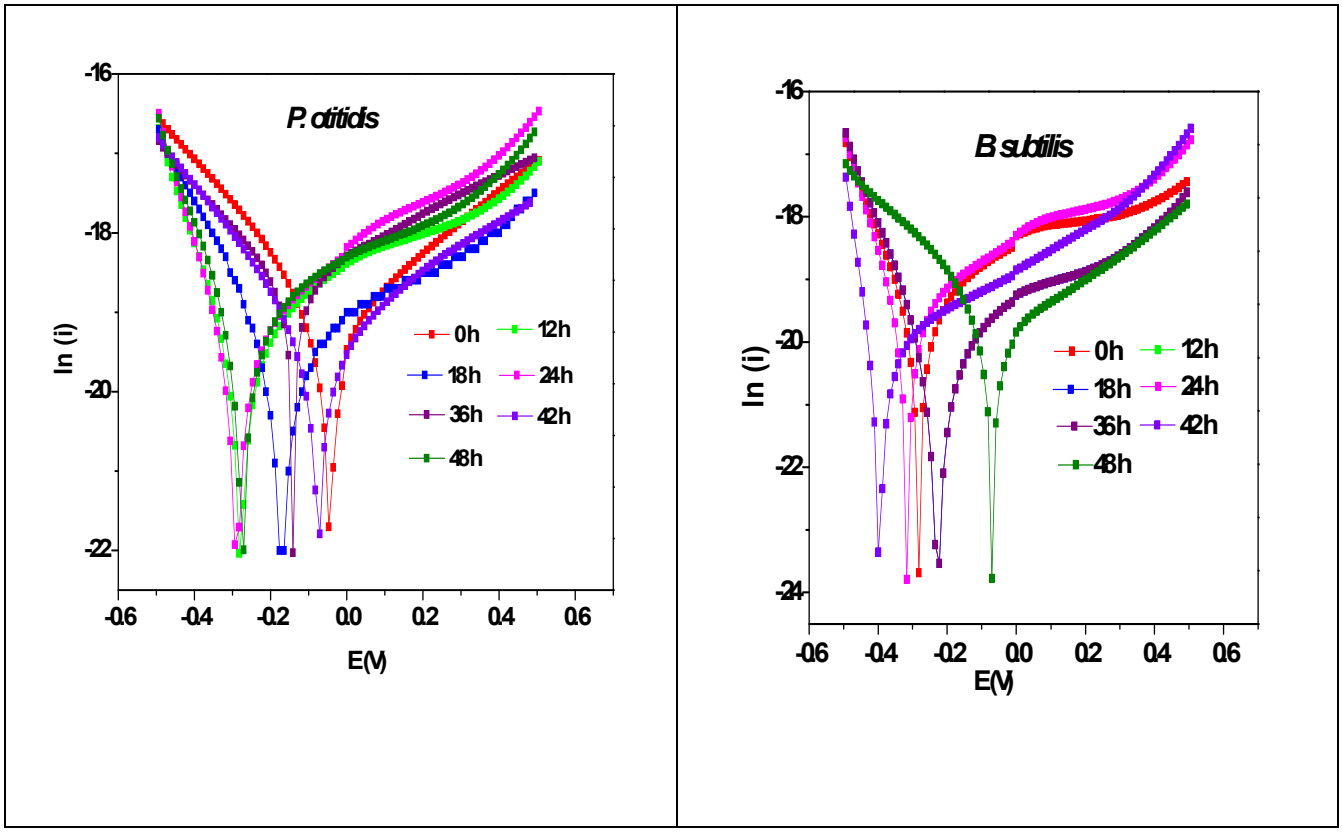
P.otitidis
ln (i)
-16
-18
-20
-22
0h
12h
18h
24h
36h
42h
48h
-0.6
-0.4
-0.2
0.0
0.2
0.4
0.6
E(V)
B.subtilis
ln (i)
-16
-18
-20
-22
-24
0h
12h
18h
24h
36h
42h
48h
-0.6
-0.4
-0.2
0.0
0.2
0.4
0.6
E(V)

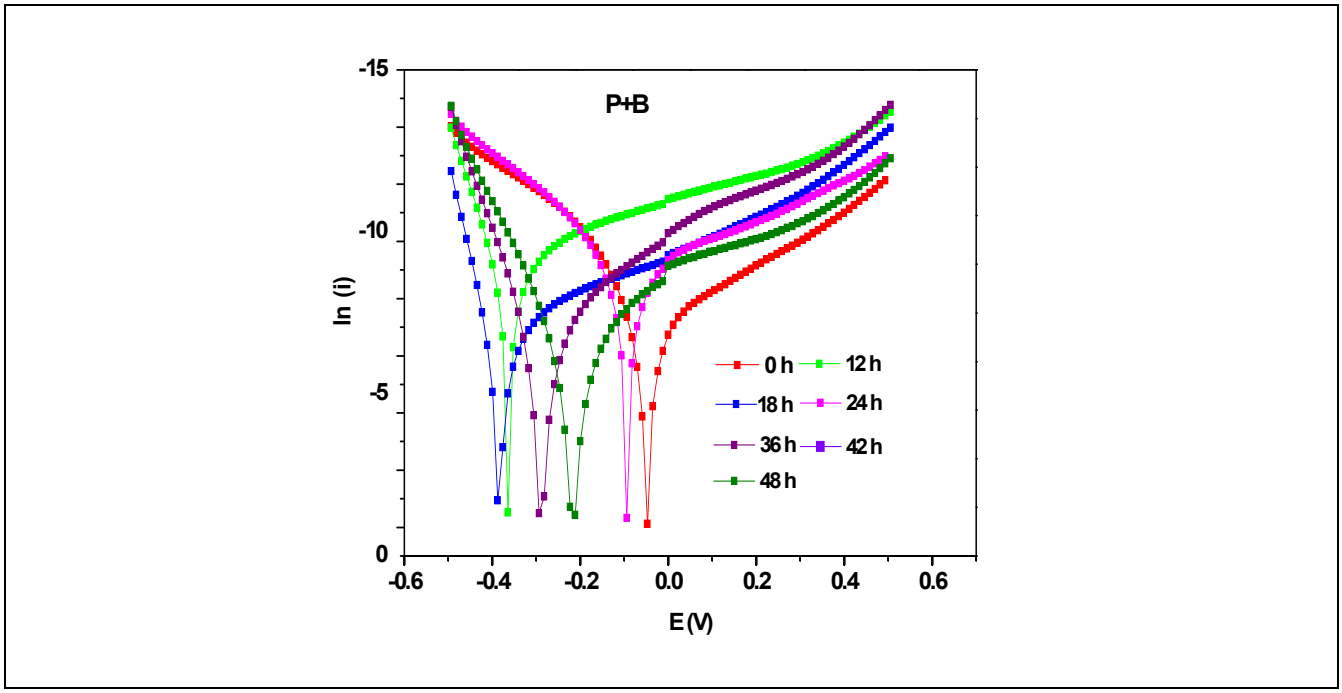
P+B
ln (i)
E(V)
0 h
12 h
18 h
24 h
36 h
42 h
48 h

Fig. 5b

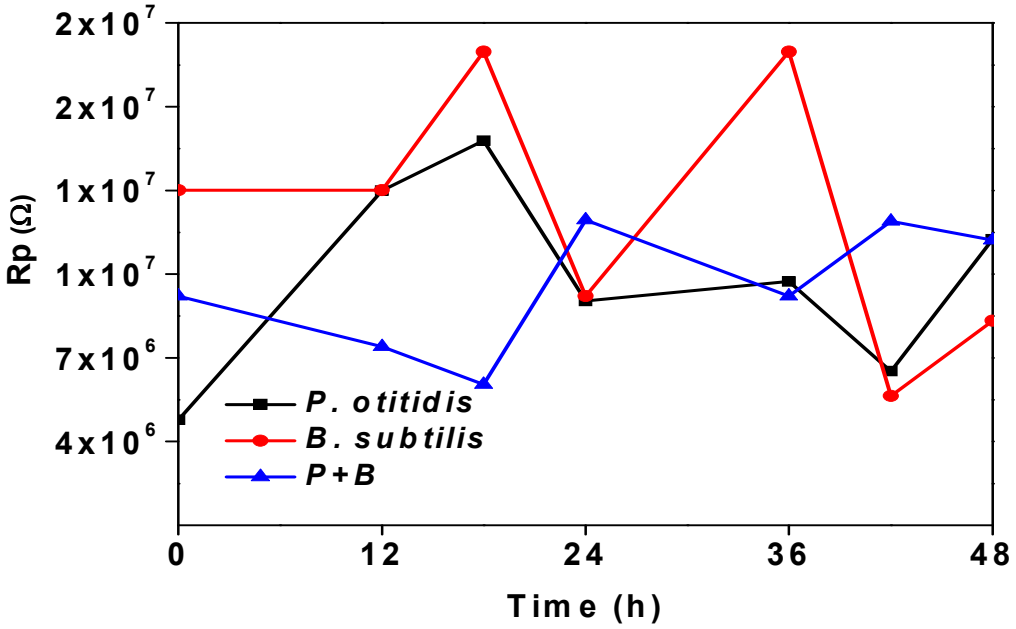
Rp (Ω)
Time (h)
P. otitidis
B. subtilis
P+B

Fig. 6

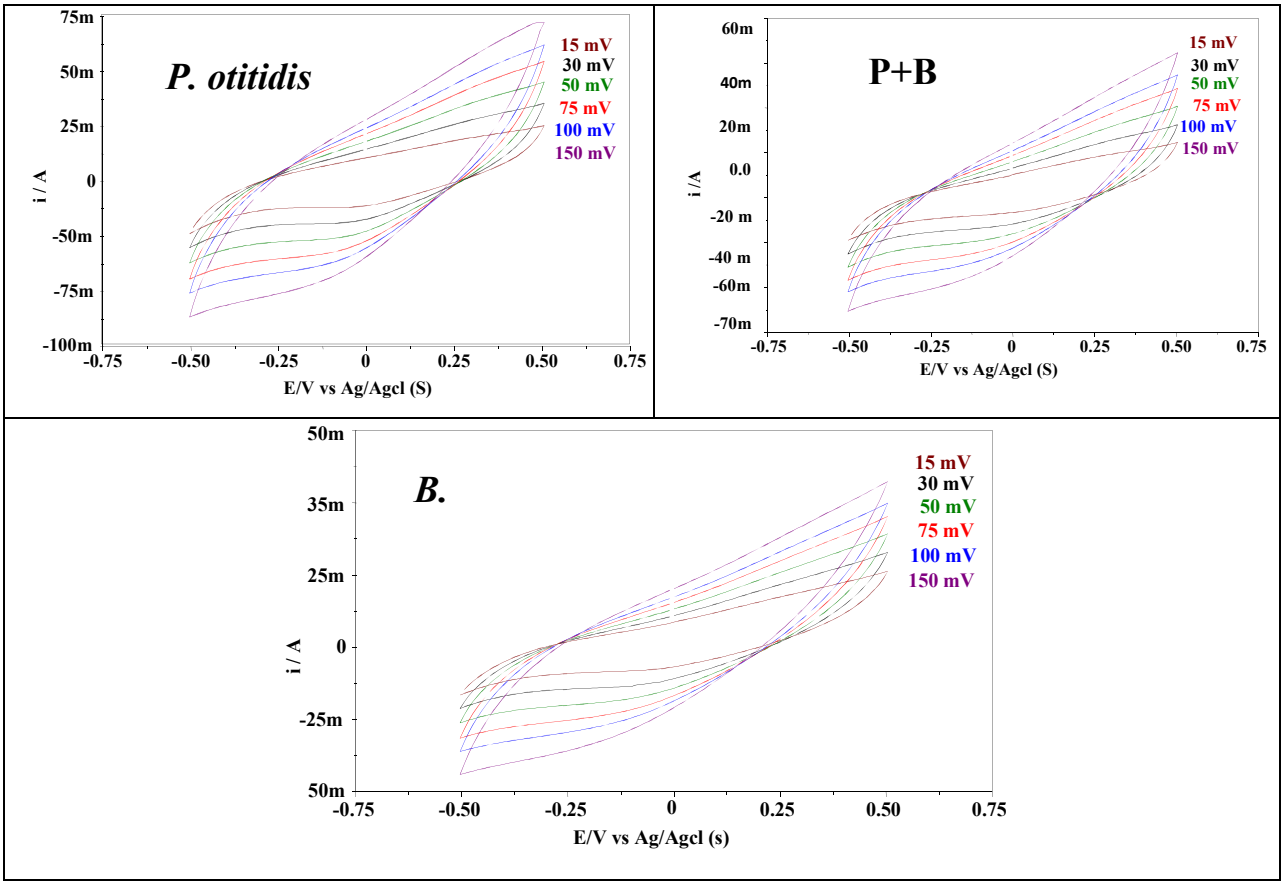
P. otitidis
15 mV
30 mV
50 mV
75 mV
100 mV
150 mV
i / A
E/V vs Ag/Agcl (S)
P+B
B.
E/V vs Ag/Agcl (s)

Fig. 7

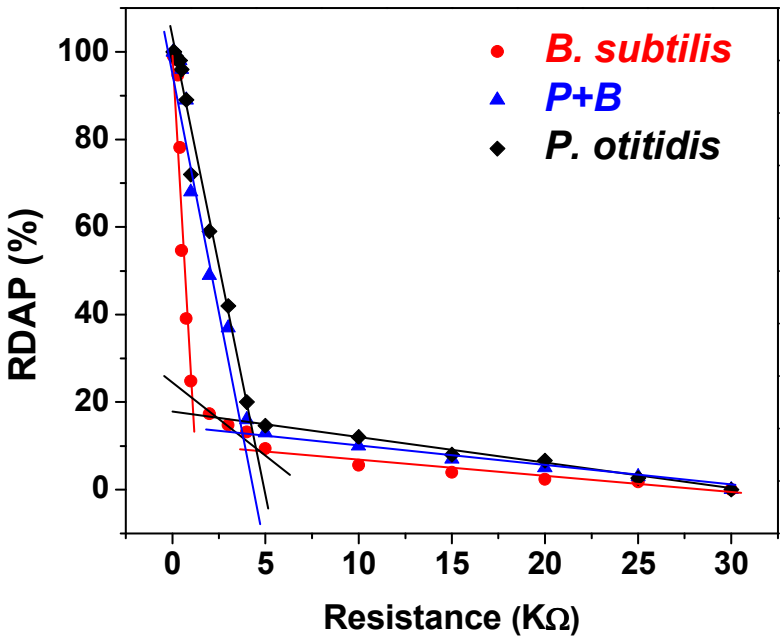
B. subtilis
P+B
P. otitidis
RDAP (%)
Resistance (KΩ)

Fig. 8

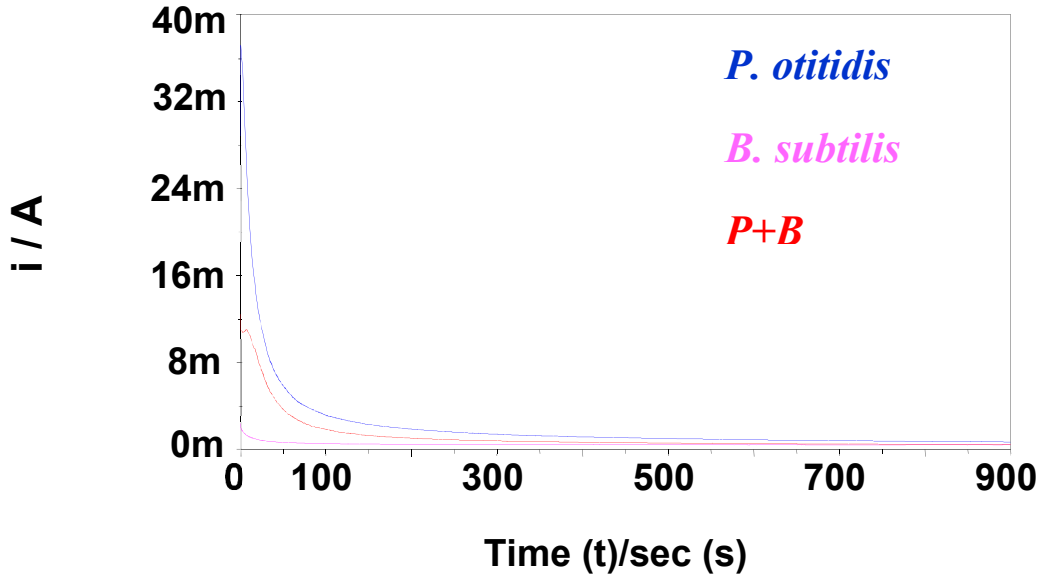
40m
32m
24m
16m
8m
0m
i / A
0
100
300
500
700
900
Time (t)/sec (s)
P. otitidis
B. subtilis
P+B

Fig. 9

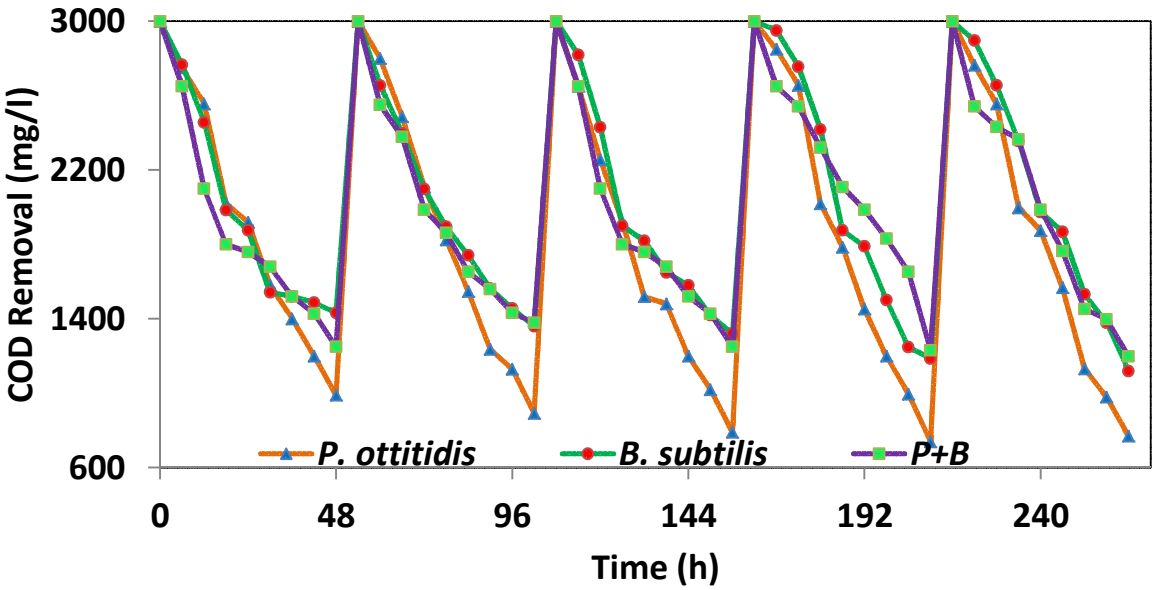
3000
2200
1400
600
COD Removal (mg/l)
0
48
96
144
192
240
Time (h)
P. ottitidis
B. subtilis
P+B

Fig. 10a

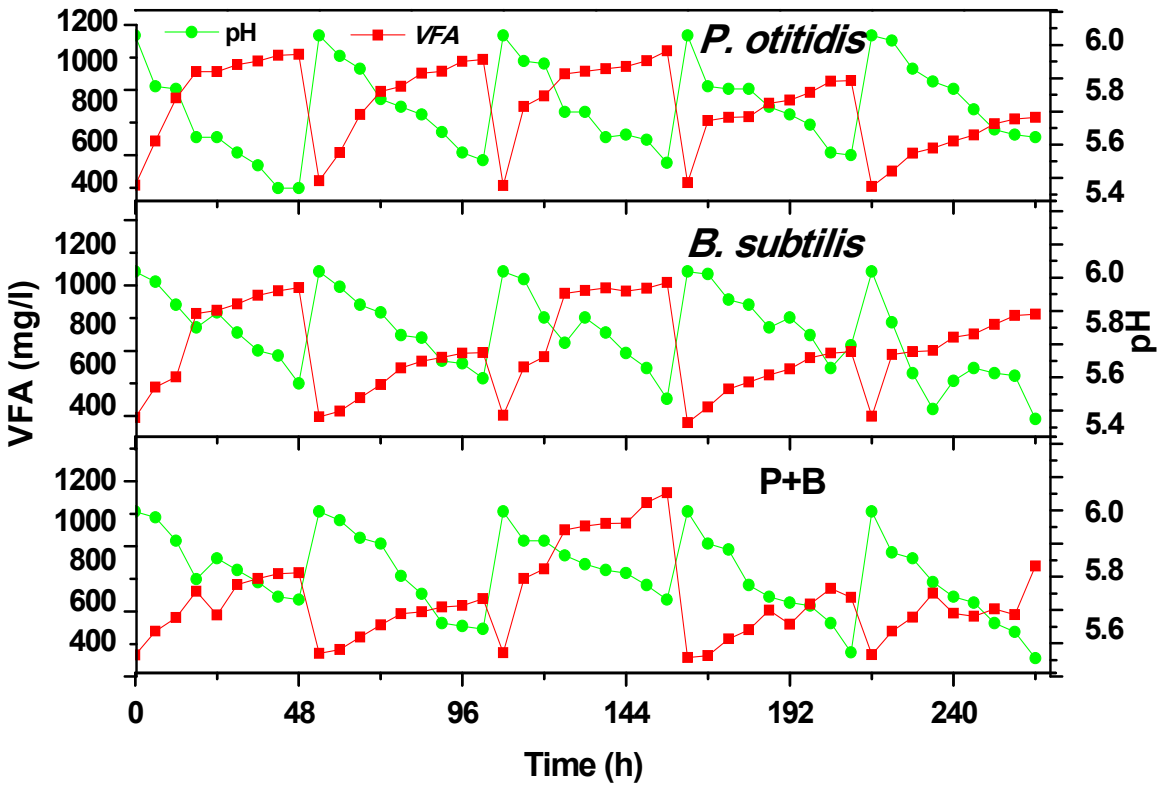
pH
VFA
P. otitidis
B. subtilis
P+B
VFA (mg/l)
pH
Time (h)
1200
1000
800
600
400
6.0
5.8
5.6
5.4
0
48
96
144
192
240

Fig. 10b